

# Stages and Kinetics of Mechanochemical Depolymerization of Poly(ethylene terephthalate) with Sodium Hydroxide

Andrew W. Tricker,<sup>†,‡</sup> Anuoluwatobi A. Osibo,<sup>†</sup> Yuchen Chang,<sup>†</sup> Jason X. Kang,<sup>†</sup> Arvind Ganesan,<sup>†</sup> Elisavet Anglou,<sup>†</sup> Fani Boukouvala,<sup>†</sup> Sankar Nair,<sup>†,‡</sup> Christopher W. Jones,<sup>†,‡</sup> Carsten Sievers <sup>\*,†,‡</sup>

<sup>†</sup>School of Chemical & Biomolecular Engineering, Georgia Institute of Technology, Atlanta, GA, 30332, USA

<sup>‡</sup>Renewable Bioproducts Institute, Georgia Institute of Technology, Atlanta, GA, 30332, USA

\*Corresponding Author; Email: carsten.sievers@chbe.gatech.edu

## KEYWORDS

Ball Milling, Hydrolysis, Mechanochemistry, Plastics Recycling, Polymers

## ABSTRACT

Efficient chemical recycling of consumer plastics (*i.e.* depolymerization down to monomers) is a crucial step needed to achieve a circular materials economy. In this work, depolymerization of poly(ethylene terephthalate) (PET) via mechanochemical hydrolysis with sodium hydroxide is studied, with complete depolymerization achieved in 20 min. The stages of the depolymerization

are investigated by monitoring monomer yields and the change in the PET molecular weight over the course of the reaction. The monomer yields initially increase linearly with milling time, up to a yield of roughly 40%. However, the molecular weights of the residual PET decrease concomitantly only slightly, suggesting a reaction scheme analogous to a shrinking core model. As the reaction progresses, a physical transition of the PET/NaOH from a powder to a homogenous wax and a simultaneous increase in the depolymerization rate is observed. The influence of ball-to-powder mass ratio (BPR) and milling frequency are studied to derive a kinetic rate expression. The linear relationship between BPR and monomer yield and the known relationship between milling frequency are validated for this system.

## INTRODUCTION

The world's production processes have historically relied on linear economies in which raw materials are processed into manufactured goods that are later discarded as waste. Consumer plastics are emblematic of the negative aspects of this model; they are sourced from unsustainable fossil resources and their resistance to decay and poor waste management pose threats to the environment.<sup>1-2</sup> It was estimated that over 359 million tons of plastics were produced globally in 2018, and this number is projected to grow at the rate of 3% annually.<sup>3</sup> Less than 10% of the total plastic ever produced has been recycled, with the majority of the plastic waste either landfilled or released into the environment.<sup>4</sup> Microplastics disperse into marine environments, cause adverse effects throughout the ecosystem and food chain, and eventually induce potential health threats to the human population.<sup>1-2</sup> In efforts to alleviate environmental strain and improve resource efficiency, there has been increasing interest in a transition to a circular economy, which is rooted

in the reuse and recycling of waste materials into intermediates that are practically identical to virgin starting materials and can be remanufactured and reprocessed.<sup>5</sup>

Poly(ethylene terephthalate) (PET) is one of the most abundant types of plastic. It is desirable due to its low cost, light weight, and excellent durability.<sup>1</sup> Its physical and chemical properties allow it to be used in a multitude of applications, especially in the textile and packaging industries.<sup>6-7</sup> In 2019, 32 million tons of PET were produced globally,<sup>8</sup> with 80% ending in landfills or the environment and a mere 10% being recycled.<sup>9</sup> Because of its non- biodegradability, PET poses a serious environmental problem, as it takes about 300 years to decompose.<sup>10</sup> Recycling PET waste can be arranged into three categories: pre-consumer recycling, post-consumer mechanical recycling, and chemical recycling.<sup>6, 11</sup> Currently, the most common recycling method is mechanical through physical reshaping processes, but mechanical recycling is limited in its effectiveness. The use of physical forces to reshape PET results in the cleaving of polymer chains that deteriorates the integrity of the material.<sup>1, 12</sup> Consequently, the plastic may only be recycled a limited number of times before its properties no longer suffice for specific applications. Furthermore, mechanically recycled PET may only be reused if mixed in with a large amount of virgin polymer, further diminishing its reusability.<sup>13</sup> Achieving widespread recycling of PET will require a more efficient process that can maintain the material properties of the virgin plastic.

Chemical recycling, although less common, has recently been the focus as a potentially promising alternative. Chemical recycling is not limited by potential shortening and degradation of polymer chains because it focuses on depolymerization into monomers and oligomers that may be purified and reconstituted into virgin materials, avoiding losses in material and mechanical properties. The most common methods of depolymerizing PET use water (hydrolysis), glycols (glycolysis), or alcohols (alcoholysis) as reagents to cleave the ester linkages.<sup>7</sup> The glycolysis

reaction involves the conversion of PET to bis(2-hydroethyl) terephthalate (BHET), in the presence of excess ethylene glycol (EG).<sup>14-15</sup> In alcoholysis, PET is broken-down to ethylene glycol (EG) and dialkyl terephthalate. Lastly, hydrolysis depolymerizes PET into monomers of terephthalic acid (TPA) and ethylene glycol (EG). Hydrolysis reactions can be done in an acidic,<sup>16</sup> neutral,<sup>17-20</sup> or alkaline<sup>11, 21-23</sup> environments. The reaction conditions for several of these processes involve high temperatures up to 250 °C. PET contamination by heavy metals and colorants, use of toxic organic solvents, low monomer yields, and challenging purification of the products are also some hurdles faced in PET depolymerization.<sup>24-25</sup>

Mechanochemical depolymerization using ball mills or similar devices is a promising approach to process solid feedstocks with a solid catalyst or reactant in an economically viable way that does not require solvents. While there are gaps in the fundamental understanding of mechanochemistry, mechanocatalytic depolymerization has been demonstrated on a lab scale for lignocellulosic biomass,<sup>26-28</sup> cellulose,<sup>27-30</sup> lignin,<sup>28, 31-33</sup> and chitin.<sup>34</sup> In addition to the ability to process solids, ball milling is a highly scalable industrial process, and its many applications include the production of several billion tons/year of cement.<sup>35</sup> Ball mills operate with electrical energy and are thus also compatible with the increasing availability of electricity from renewable sources. Mechanochemistry thus has many advantages over other unconventional approaches such as biological depolymerization by microbes/enzymes, which must overcome challenges in productivity, resistance to contaminants, and separations, especially when handling mixed-waste feedstocks.<sup>36-37</sup>

The study of mechanochemically depolymerization of PET is still in its infancy. Li *et. al* demonstrated greater than 80% conversion of PET via high temperature (270 °C) reactive melt processing with Ca(OH)<sub>2</sub> using a roller mill, followed by treatment in 100 °C water,<sup>38-39</sup> and Štrukil

reported the quantitative mechanochemical hydrolysis of PET with NaOH using a vibratory ball mill at room temperature.<sup>40</sup> Several reaction parameters were explored by Štrukil, including strength of the base, milling intensity, liquid assisted grinding, and inclusion of mixed polymers. However, a systematic quantitative exploration of the dependency of these (and more) reaction parameters on the depolymerization rate is still needed to gain the ability to predict mechanochemical depolymerization processes.

In this work, the kinetics of the mechanochemical reaction of PET and NaOH are systematically studied in a ball mill reactor. The physical transition of the reactants from a powder to a waxy substance is discussed, and the impact of this transition on the depolymerization reaction is analyzed. In addition, the effects of thermal (i.e., heat) and mechanical energy (i.e., kinetic energy of balls) supply are analyzed and quantitative descriptors are proposed.

## EXPERIMENTAL SECTION

### Chemicals

Poly(ethylene terephthalate) (PET) pellets were supplied by PolyQuest Inc. Sodium hydroxide (>97%), ethylene glycol (>99%), bis(2-hydroxyethyl) terephthalate (98%), terephthalic acid (98%), 1,1,1,3,3-hexafloro-2-propanol (>98%), methanol (>99.9%), and deuterium oxide (98%) were purchased from Sigma-Aldrich. Disodium terephthalate (99+) was purchased from Alfa Aesar. Mono-(2-hydroxyethyl) terephthalate (MHET) (97%) was purchased from AchemBlock. Sodium trifluoroacetate (98%) was purchased from Thermo Fisher Scientific. PET calibration standards for gel permeation chromatography analysis were purchased from American Polymer Standards Corporation. Further purification of each of these chemicals was not performed.

## **Mechanochemical Reactions**

Mechanochemical hydrolysis reactions with PET and sodium hydroxide (NaOH) were performed using a Retsch MM400 ball mill. Experiments studying the depolymerization kinetics by varying milling frequency, ball mass, or vessel temperature used 1.0 g of PET, 0.42 g of NaOH, a 25 mL stainless steel vessel, and a 20 mm diameter grinding ball. Either a stainless steel (S.S.), tungsten carbide (WC), or aluminum oxide ( $\text{Al}_2\text{O}_3$ ) ball was used to change the mass of the ball and keep a constant diameter. Experiments studying the influence of the ball-to-powder ratio used a 25 mL stainless steel vessel and stainless-steel grinding balls with diameters of 7 mm, 12 mm, 15 mm, or 20 mm. PET loadings were varied from 0.05 g - 5 g. Unless otherwise stated, PET was milled with stoichiometric amounts of NaOH. A separate experiment was conducted for each time point to prevent interference of the reaction by stopping milling or opening the vessel.

Non-ambient depolymerization reactions were conducted by either cooling the milling vessel with liquid nitrogen or heating the milling vessel with heating tape. For the sub-ambient temperature reactions, the milling vessel was submerged in liquid nitrogen for 5 min before the reaction and then liquid nitrogen was continuously poured over the vessel during milling. The external temperature of the vessel was maintained at  $-35 \pm 5^\circ\text{C}$ . For elevated temperature reactions, the vessel was wrapped in heating tape during the course of the reaction. The temperature was maintained at  $92 \pm 7^\circ\text{C}$ .

## **High Performance Liquid Chromatography (HPLC)**

Yields of disodium terephthalate ( $\text{Na}_2\text{TPA}$ ) and sodium mono-(2-hydroxyethyl) terephthalate ( $\text{NaMHET}$ ) were determined via high performance liquid chromatography (HPLC) (Agilent 1260 Infinity Series with a UV detector set to 242 nm). The analysis was performed with a Poroshell

120 SB-C18 column under gradient flow from 70% 0.1 wt% H<sub>3</sub>PO<sub>4</sub> in water and 30% methanol to 10% 0.1 wt% H<sub>3</sub>PO<sub>4</sub> in water and 90% methanol. The instrument was calibrated with 1 mg/mL stock solutions of terephthalic acid (TPA) and mono-(2-hydroxyethyl) terephthalate (MHET) in methanol. Each stock solution was diluted 10 times with water to a sample concentration of 0.1 mg/mL. Then, 10-100  $\mu$ L of the solution was pipetted into a centrifuge tube containing 300  $\mu$ L of pure methanol and 700  $\mu$ L of 0.1wt% H<sub>3</sub>PO<sub>4</sub>.

After the reaction time, between 1 and 10 mg of a solid sample was placed into a centrifuge tube and diluted with 1 mL of DI water (**Solution 1**). The sample was then vortexed and sonicated for 30-45 min and placed overnight for insoluble residues to sediment completely. Experiments emphasizing product selectivity were neutralized with the following work-up procedure within 10 min to prevent additional hydrolysis of NaMHET to Na<sub>2</sub>TPA: 10  $\mu$ L of **Solution 1** was pipetted in another centrifuge tube filled with 1 mL of DI water (**Solution 2**). Then, 100  $\mu$ L of **Solution 2**, 600  $\mu$ L 0.1wt% H<sub>3</sub>PO<sub>4</sub> in water, and 300  $\mu$ L MeOH were pipetted into an empty centrifuge tube. The solution is then filtered into an HPLC sample vial through a 0.2  $\mu$ m PTFE syringe.

Yields of products were defined as the ratio of the moles of the product (i.e., Na<sub>2</sub>TPA or NaMHET) to the moles of PET in the beginning of the reaction (assuming a molar mass of 192 g/mol) (**Equation 1**). The conversion of PET was defined as one minus the yields of the terephthalate products (**Equation 2**). The selectivity of a product (either Na<sub>2</sub>TPA or NaMHET) was defined as the yield of the product divided by the total yield of Na<sub>2</sub>TPA and NaMHET (**Equation 3**)

$$Y_{product} = \frac{n_{product,f}}{n_{PET,0}} \quad (1)$$

$$X_{PET} = 1 - \sum Y_{terephthalates} \quad (2)$$

$$S_{product} = \frac{Y_{product}}{Y_{Na2TPA} + Y_{NaMHET}} \quad (3)$$

### Gel Permeation Chromatography (GPC)

The molecular weight distribution of the PET residues was characterized by gel permeation chromatography (GPC) using a TOSOH EcoSEC Elite HLC – 8420 GPC equipped with a differential refractive index (RI) detector and a PL HFIPgel column. An eluent stream of 1,1,1,3,3,3 hexafluoropropanol (HFIP) containing 5 mM of sodium trifluoroacetate was used. The GPC was operated at a temperature of 40 °C, a flow rate of 0.1 mL/min, and an injection volume of 30 µL. GPC calibration was performed using three PET standards (Table 1).

**Table 1.** Molecular weights of PET calibration standards.

	Mn [g mol <sup>-1</sup> ]	Mw [g mol <sup>-1</sup> ]
<b>MW Std 1</b>	30,000	63,500
<b>MW Std 2</b>	21,000	39,000
<b>MW Std 3</b>	860	1155

To analyze the molecular mass of residual PET after reaction, the products from the ball mill vessel were washed with water and stirred at room temperature for 5 min to remove monomers and NaOH prior to the molecular weight analysis. The samples were then filtered and left to dry for a day. Next, 0.5 mg of the filtered solid residue was dissolved in 1mL of HFIP and sonicated for 30 min. After the sample preparation, the solution was filtered into a GPC vial using a 0.2 µm PTFE syringe filter.

## Nuclear Magnetic Resonance (NMR) Spectroscopy

After the depolymerization reaction, ~10 mg of the PET/NaOH mixture was added to 1 mL of D<sub>2</sub>O. <sup>1</sup>H NMR spectroscopy experiments were performed using a Bruker Avance III 500 MHz instrument. Spectra were collected between  $\delta_H = -3.8$  ppm and  $\delta_H = 16.2$  pm, with 16 scans per spectrum. Spectra were calibrated to the residual water peak at  $\delta_H = 4.8$  ppm.

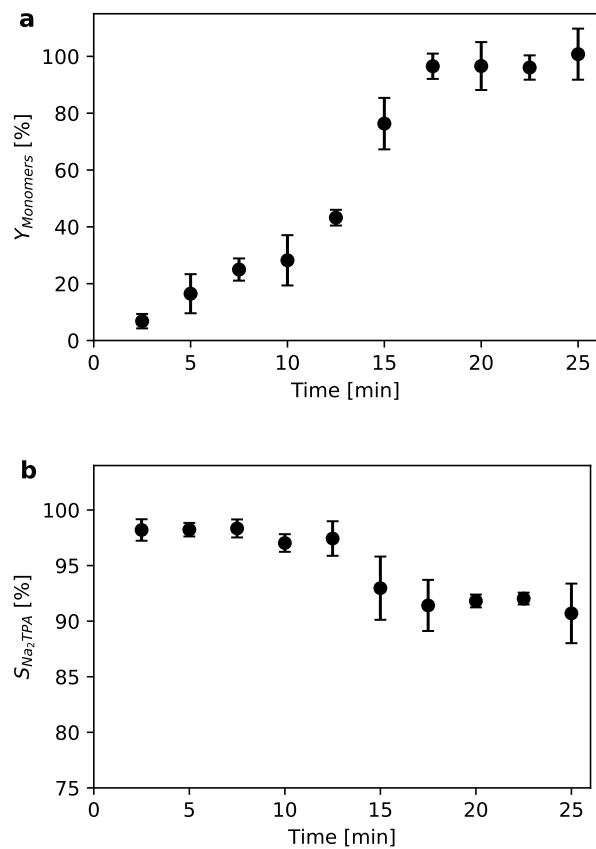
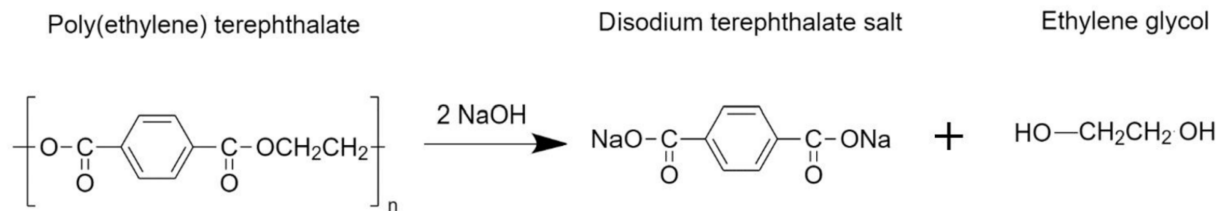
## RESULTS

### Progression of Mechanochemical PET Depolymerization

The progression of the mechanochemical hydrolysis of poly(ethylene terephthalate) (PET) (**Scheme 1**) was initially studied under a baseline condition. The monomer yield of PET was determined based on the cumulative yield of terephthalates, as determined by high performance liquid chromatography (HPLC) (**Figure 1a**). Stoichiometric yields of disodium terephthalic acid (Na<sub>2</sub>TPA) and ethylene glycol (EG) were confirmed by <sup>1</sup>H NMR spectroscopy (**Figure S1**). Additionally, elemental analysis of a sample after milling showed only ppm levels of iron and chromium, the two most abundant elements in stainless-steel of the ball and milling vessel, suggesting minimal additional contamination of the final product occurs through this process (**Table S1**). The monomer yield of PET initially increased linearly with milling time ( $t \leq 12.5$  min). An inflection point was observed after 12.5 min, where the depolymerization rate drastically accelerated. Nearly 60% of the original feedstock was depolymerized within the subsequent 5 min. This inflection point corresponded to the transition of the PET/NaOH powder (**Figure 1c**) into a homogenous waxy substance (**Figure 1d**) that stuck to the vessel walls and milling balls. Complete depolymerization occurred within 17.5 min. Štrukil reported a 51% monomer yield at 30 min,<sup>40</sup>

however this lower monomer yield is not unexpected considering the smaller 12 mm ball used in those experiments compared to the 20 mm ball in this work.

**Scheme 1.** Alkaline hydrolysis of poly(ethylene terephthalate) (PET)



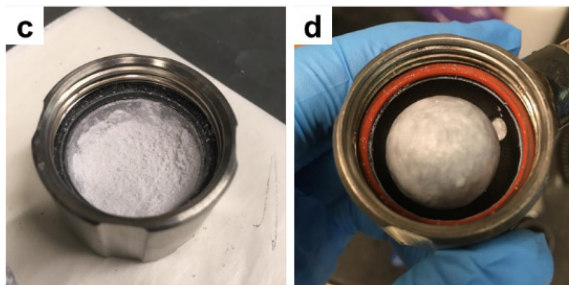


**Figure 1.** Mechanocomical reaction of PET with NaOH with 1.00 g of PET, a stoichiometric amount of sodium hydroxide (NaOH), one 20 mm stainless steel milling ball, and a milling frequency of 30 Hz: a) Monomer yields, b) Na<sub>2</sub>TPA selectivity, c) Picture of PET and NaOH powder d) Picture of waxy substance coated on the milling ball. Error bars are standard deviation of three trials.

During depolymerization, Na<sub>2</sub>TPA was the primary product, while small yields of sodium mono-(2-hydroxyethyl) terephthalate (NaMHET) were observed. The highest selectivity (98%) of Na<sub>2</sub>TPA was observed at low yield, with the selectivity decreasing to 91% at full depolymerization (**Figure 1b**). The sample was milled for an additional 7.5 min after full depolymerization occurred, but the yield of NaMHET did not change. In a single run, the PET/NaOH was milled in the presence of 100  $\mu$ L of EG (0.34 equiv.) for 10 min. The presence of EG increased the monomer yield from 30% to 47%, but the mixture remained a powder. Additionally, the selectivity of NaMHET rose drastically to 20%, compared to just 2.6% at a similar yield under dry conditions. These results suggest that the NaMHET can form from a reaction between disodium terephthalate and EG, and that NaOH may be able to act as a glycolysis or alcoholysis catalyst.

The changes in the weight average molecular weight (M<sub>w</sub>), number average molecular weight (M<sub>n</sub>), and polydispersity index (PDI) of the residual PET were investigated for milling times up to 12.5 min (**Figure 2a**). For samples milled longer than 15 min, recoverable yields of PET were too low to reliably analyze with GPC (**Figure S2**). The average M<sub>w</sub> of the residual PET residues

decreased slightly in the first 7.5 min of the reaction from 52,800 g mol<sup>-1</sup> to 50,100 g mol<sup>-1</sup>, and then a more significant reduction to 43,700 g/mol was observed over the next 7.5 min. The changes in Mn values were less significant, decreasing from the initial value of 27,100 g mol<sup>-1</sup> to 26,000 g mol<sup>-1</sup>. The molecular weight distributions (MWD) of the residual polymer samples were analyzed in more detail (**Figure 2b**). As evidenced by the decreasing PDI, the MWD curves became narrower as the contributions from the longest and shortest polymer chains decreased with increasing milling time. These observations indicate that some of the largest polymers are cleaved into smaller ones, while most of the residual polymer chains were not affected.

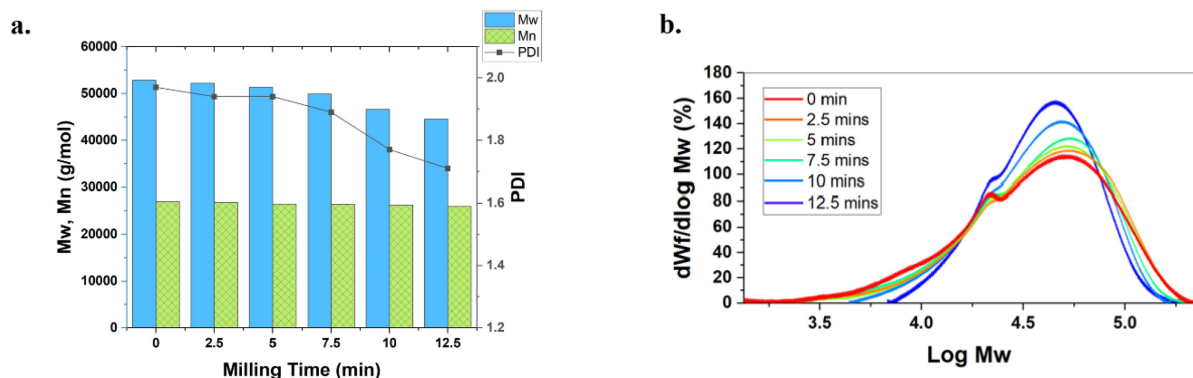


**Figure 2.** GPC results of residual PET after milling with NaOH: 1 g of PET milled with 0.42 g of NaOH at 30 Hz and 20 mm S.S ball (a) Mw, Mn, and PDI values and (b) MWD curves of residual PET samples after mechanochemical depolymerization.

### Influence of Mechanical and Thermal Energy Supply

To understand the impact of different forms of energy supply on PET depolymerization, the most important process parameters (i.e., frequency, ball mass, vessel temperature, and ball-to-powder ratio) were varied systematically. In general, the monomer yield profiles for these conditions followed closely with the baseline case: a constant depolymerization rate at low yield followed by a sharp increase in the monomer yield after the transition from a powder to a waxy substance.

As expected, the Na<sub>2</sub>TPA yield increased with increasing milling frequency (**Figure 3a**). Milling at 30 Hz resulted in complete depolymerization within 20 min, while 25 min of milling was required to achieve 100% monomer yield at 27.5 Hz. When the same reaction mixture was milled at 25 Hz, the transition to the waxy phase did not occur until 35 min, and 100% monomer yield was obtained by 40 min.

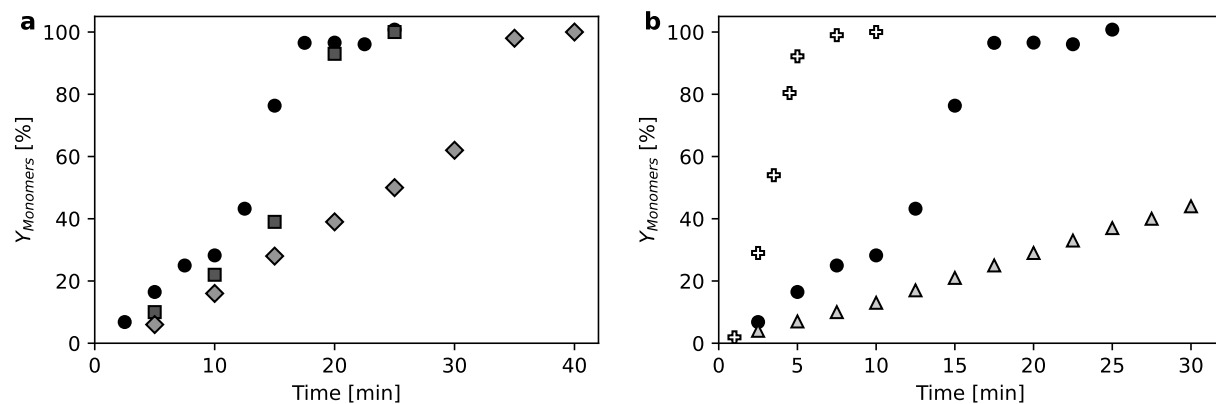


**Figure 3.** (a) Monomer yields over time at 30 Hz (●) 27.5 Hz (■), and 25 Hz (◆) with a stainless-steel grinding ball. (b) Monomer yields over time using a stainless-steel (●), tungsten carbide (✚), and aluminum oxide (▲) grinding ball at 30 Hz. (1.0 g PET, 0.42 g (1.0 equiv.) NaOH, 1 x 20mm ball, 25 mL stainless-steel milling vessel

To probe the influence of the mass of the milling ball, the depolymerization reaction was carried out with a tungsten carbide (WC,  $\rho = 15.6 \text{ g cm}^{-3}$ ,  $m_{ball} = 61.7 \text{ g}$ ) and an aluminum oxide ball ( $\text{Al}_2\text{O}_3$ ,  $\rho = 3.95 \text{ g cm}^{-3}$ ,  $m_{ball} = 16.2 \text{ g}$ ), along with the stainless-steel ball (S.S.,  $\rho = 7.5 \text{ g cm}^{-3}$ ,  $m_{ball} = 32.2 \text{ g}$ ) used in the baseline experiments (**Figure 3b**). Changing the ball material allowed for varying the mass of the ball while the diameter remained constant (20 mm). Full depolymerization was reached within 7.5 min when milling with the WC ball, compared to 20 min using the S.S. ball. Notably, during reaction with the WC ball, the temperature of the milling vessel increased to 50 °C, which is 20 °C higher than during the reaction with the S.S. ball. However, the

bulk reactor temperature is not expected to play a significant role in the depolymerization rate (see below). In the reaction with the  $\text{Al}_2\text{O}_3$  ball, the yield after 30 min was only 45% and the reaction mixture remained a powder.

Experiments with heated and cooled milling vessels were performed to analyze the influence of thermal and mechanical energy on the PET depolymerization reaction (**Figure 4**). Without active heating or cooling, the stainless-steel vessel will internally heat to approximately 30 °C when milling at 30 Hz with the single 20 mm S.S. ball within about 5 min. For cooling, the ball mill reactor temperature was kept at  $-35\pm 5$  °C by continually flowing liquid nitrogen on the milling vessel, and repeatedly immersing it in liquid nitrogen every 5 min. Throughout the course of the reaction, there was no formation of a waxy phase, and the monomer yield after 25 min was only 42%. The milling vessel was also heated to  $92\pm 7$  °C, which is above the glass transition temperature of PET (78 °C), using heating tape. There was an early-onset form of wax (after 5 min), which is attributed to the transition of the PET from a glassy state to a rubbery state. However, there was only a marginal increase in the monomer yield for this experiment compared to milling at room temperature.

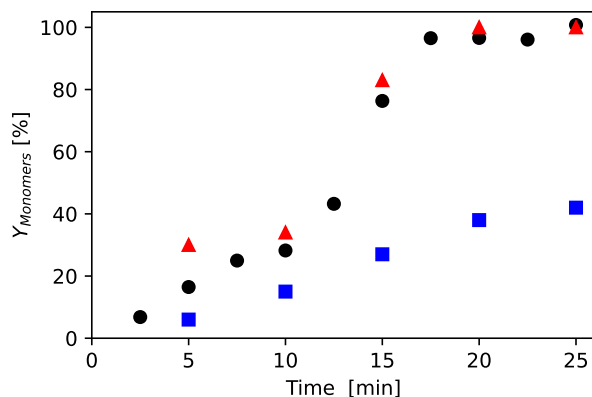


**Figure 4.** Monomer yields over time at  $\sim 30$  °C (●),  $92 \pm 7$  °C (▲), and  $-35 \pm 5$  °C (■). (1x20 mm S.S. ball, 30 Hz, 1.0 g PET, 0.42 g (1.0 equiv.) NaOH, 25 mL S.S. vessel)

In addition to independent variables like ball mass and milling frequency, lumped parameters can be used to study how mechanical forces trigger reactions.<sup>41-42</sup> A common lumped parameter that can be used to compare PET data for various ball sizes and loadings is the ball-to-powder ratio (BPR),<sup>43</sup> which is the ratio of the total ball mass to the mass of substrates (PET + NaOH) (**Equation 5**). The influence of the BPR was studied by measuring the monomer yield at 20 min and 30 Hz for BPR values ranging from ~5 to ~45. The BPR values were adjusted by either changing the diameter of the stainless-steel grinding ball (from 7 mm up to 20 mm) or changing the mass of reagents. For context, the baseline condition (**Figure 1**) had a BPR of 22.7 and the depolymerization experiments with the WC and Al<sub>2</sub>O<sub>3</sub> balls (**Figure 3b**) had BPR values of 43.5 and 11.2, respectively. Regardless of ball size, it was found that monomer yield as a function of the BPR collapsed into a single curve (**Figure 5**), with three distinct regimes. For BPR  $\geq 20$ , full depolymerization of PET to Na<sub>2</sub>TPA was reached by 20 minutes. For BPR values between approximately 10 and 20, the monomer yield of Na<sub>2</sub>TPA increased linearly with BPR. At BPR  $\sim 10$ , an inflection point was observed where the slope of the relationship between BPR and Na<sub>2</sub>TPA decreased significantly. This transition is ascribed to a transition in the limiting phenomena for the depolymerization reaction. Below a BPR of 10, coarser PET and NaOH particles were observed after milling, suggesting the reaction could have been limited by available surface area. Above a BPR of 10, the powder was significantly finer and the reaction is anticipated to be controlled by the energy transfer from the milling to the powder.

$$BPR = \frac{m_{ball}}{m_{substrate}} \quad (5)$$

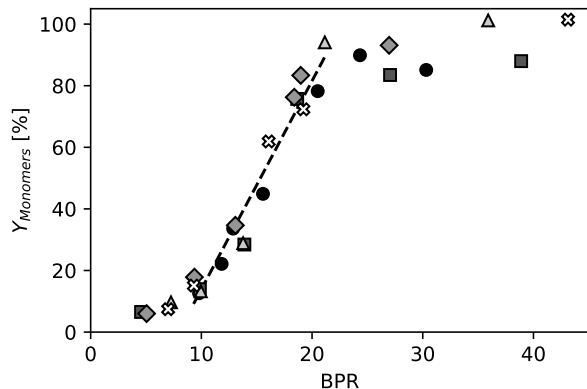


**Figure 5.** Monomer yields as a function of BPR for single ball milling experiments using one 20 mm ball (●,  $m_{\text{ball}} = 32.2$  g), 15 mm ball (■,  $m_{\text{ball}} = 13.4$  g), 12 mm ball (◆,  $m_{\text{ball}} = 6.9$  g), 10 mm ball (▲,  $m_{\text{ball}} = 4.0$  g), or 7 mm ball (◆,  $m_{\text{ball}} = 1.4$  g). The dashed line shows best linear fit for  $20 \gtrsim \text{BPR} \gtrsim 10$  for all runs. Reagents milled in a 25 mL stainless steel vessel for 20 minutes at 30 Hz.

## DISCUSSION

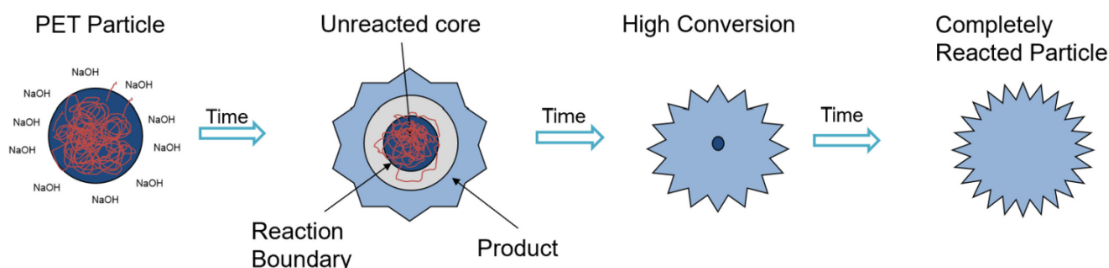
### Stages of the Depolymerization Process

The kinetics of step polymerization, which is the mechanism of PET polymerization, are characterized by the rapid and near complete consumption of monomers before the production of any medium or large molecular weight polymers.<sup>44</sup> However, the present study shows that mechanochemical depolymerization of PET with NaOH occurs via a reaction path that is distinct from the reverse of step polymerization. Specifically, the steady increase of the monomer yields with increasing milling time and the limited changes of the molecular weight distribution show that certain polymer chains are depolymerized entirely while others are barely affected. The mechanochemical alkaline hydrolysis of PET can be conceptually described by a shrinking core model (**Scheme 2a**), much like aqueous alkaline PET depolymerization.<sup>45-46</sup> In this model, the PET domains remain a distinct phase from the NaOH, so that only the outmost layer of polymer chains

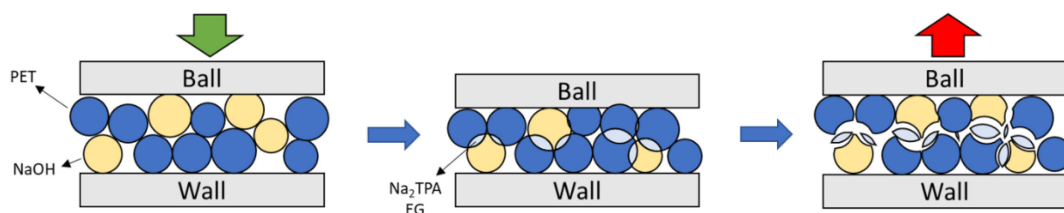
on the surface of the PET particle can be exposed to reactive conditions. During milling, the NaOH must react within an activated zone at the outside of the particle to fully convert the PET in this volume to Na<sub>2</sub>TPA and EG, as evidenced by the high selectivity towards Na<sub>2</sub>TPA over the whole course of depolymerization. Since the average molecular weight of residual polymer chains remains approximately unchanged, even up to high conversions, the PET chains below this reactive zone cannot be meaningfully affected. As the reaction progresses with time, remaining particles of unreacted PET shrink until full conversion is reached.

**Scheme 2.** Reaction progression of PET depolymerization (a) analogous to shrinking core model and (b) dependent on the forced area of contact of the reactants by collision.

**a.**



**b.**



The traditional solid-fluid interface based shrinking core model describes the reaction rate based on a concentration gradient of reactant from a homogenous fluid to the solid surface.<sup>47</sup> In the mechanochemical hydrolysis of PET, a concentration gradient is not expected to be the primary determinant for the reaction rate. Rather, the energy of the milling would ultimately be expected

to determine the rate by controlling how much NaOH can reach PET during collision and the energetics of the collision/reaction environment. Importantly, the NaOH and depolymerization products do not necessarily form a homogenous mixture as depicted in **Scheme 2a**. The NaOH could instead remain as distinct particles, where the reactive front is better described as the forced contact area of the PET and NaOH particles by the collision (**Scheme 2b**). Qualitatively, these two framings are the same, and the reality in the milling vessel is mostly like a combination of the two where the NaOH remains separate particles, but the PET is coated in a mixture of NaOH, Na<sub>2</sub>TPA, and EG.

The independence of the reaction rate with respect to monomer yield, while the substrate remained a powder, was observed for all cases when varying milling frequency and ball mass. In a conventional shrinking core model, the reaction rate is expected to be dependent on the surface area of the PET and the concentration of NaOH. In typical shrinking core models, particles are assumed to be spheres with a decreasing radius as conversion increases. However, the milling action on the PET particles can instead deform and fracture particles. Non-uniform reaction rates around the PET surface would also result in non-spherical particles, leading to increasing surface area as the reaction progresses. With respect to the concentration of NaOH, the NaOH could be considered in molar excess up to relatively high conversions, since the molar density of NaOH is nearly ten times that of PET. This high local concentration could result in a rate that is pseudo-zero order with respect to NaOH. If the NaOH does not homogenize with the products, then the rate would depend on the surface area of NaOH and a similar argument could follow as with the PET surface area. A final possibility could be changes in the interactions between the milling ball and the substrate as the physical properties of the powder change with depolymerization, as indicated by the formation of the wax and rapid depolymerization at higher Na<sub>2</sub>TPA yield. The

energy could be transferred more efficiently, resulting in more energetic reaction conditions and greater interaction of the PET and NaOH. The exact contributions of these phenomena, as well as potentially others, to the reaction rate cannot be determined from the current data set but should be the focus of follow-up work.

The inflection point in the rate of depolymerization generally corresponded to a transition of the reactant and product mixture from a powder into a homogenous waxy phase. A similar sigmoidal conversion curve and formation of a rubbery substrate was observed during the mechanochemical Knoevenagel condensation of vanillin and barbituric acid.<sup>48</sup> In that work, the interplay between the sigmoidal kinetics and cohesive state was attributed to a feedback loop between the reaction progression/chemical kinetics and the material rheology. Specifically, the authors postulated the change in kinetics results from the significant increase in vessel temperature when milling a rubbery material compared to a powder. An important distinction between these systems is the presence of large macromolecules in the current work, as opposed to smaller organic molecules, which introduce several additional complexities.

Milling is expected to decrease the crystallinity of the PET,<sup>49</sup> which in turn is expected to decrease the chemical resistance of the plastic.<sup>50</sup> The combination of mechanical stresses and degradation of the PET particles could result in a critical conversion where the PET polymers become disentangled, creating a pseudo-solution of polymer and product. Here, the polymer chains become much more accessible to the NaOH, resulting in rapid depolymerization. However, the deconvolution of wax formation and accelerated yield at elevated temperatures suggests that while the polymer rheology plays a role in the wax formation, additional phenomena influence the monomer yield rate. The inflection point was observed around similar extents of reaction at the elevated temperature and ambient temperature, so one of the products may autocatalyze the

reaction. For example, ethylene glycol may partially solubilize the NaOH, facilitating access to the PET ether bonds.

The rheology of the wax mixture should still play a significant role, too. The wax is expected to behave like a highly viscous material compared to the more ridged PET and NaOH particles. The viscoelastic nature of the wax can result in more inelastic collisions and increase the energy transfer per collision. The remaining reactants can also concentrate around the milling ball or milling vessel. The random displacement of the reactants in the milling vessel decreases, and the rate of effective collisions between the ball and the PET increases. Of course, future work will be necessary to elucidate the precise phenomena that initiate the wax formation and the reasons for the rapid depolymerization.

Since an essentially quantitative monomer yield was obtained, there is no reason to doubt that the product can be repolymerized after appropriate workup. Even though the depolymerization is performed in a solid-state, downstream separation process would require solvents and solid adsorbents. An efficient separation system would recover monomers using recyclable (low-boiling) and environmentally friendly solvents and also remove impurities/additives by processes such as adsorption. Details of the separation system along with overall process modeling and technoeconomic analysis will be presented in our forthcoming work.

### **Influence of Thermal Energy**

The mechanocatalytic depolymerization reaction of PET was operated at very low and high temperatures. The temperature can affect the rate constant for the depolymerization reaction according to Arrhenius law but also affects the material properties of polymers and thus the way that they absorb mechanical impact. PET is more brittle at low temperatures,<sup>51</sup> and it was

hypothesized that this would increase the effectiveness at which mechanical energy can drive the depolymerization reaction. However, compared to milling at ambient conditions, the yields of Na<sub>2</sub>TPA were lower when the vessel was cooled to -35 °C (**Figure 4**). A possible explanation for this is that the added mechanical energy was not sufficient to compensate the thermal contribution toward overcoming the activation barrier of the reaction. Additionally, this reaction temperature is below the freezing point of ethylene glycol (-12.9 °C). As such, the reaction could also be limited by the exchange of Na<sub>2</sub>TPA and EG with fresh NaOH at the PET surface.

When there was a significant increase in the heat energy, the PET depolymerization rate was expected to increase significantly. However, this was not the experimental observation. This may be because of the presence of the rubbery form of PET at temperatures above 78 °C. Consequently, the PET may behave more like a viscous liquid rather than a compressible powder under impact at these conditions, resulting in a greater area of energy dissipation and potentially changing the modes of energy transfer from the ball.

### Depolymerization Kinetics and Energy Dose

Just like conventional reactors, understanding the kinetics of the mechanochemical process is essential for predicting the desired reaction pathway, critical for controlling a reaction, and ultimately evaluating efficiencies at larger scales. The kinetics of a reaction environment are governed by the energetic descriptor of the system, such as temperature in thermochemical reactions or potential in electrochemical reactions. In mechanochemical reactions, the milling intensity ( $I_m$ ), the energy transferred from the ball per mass of substrate per unit of time, has been shown to be a useful energetic descriptor when measuring mechanochemical kinetics.<sup>52</sup> Therefore, the reaction rate is expected to be proportional to the milling intensity (**Equation 5**). While the exact value can be highly dependent on system specifics,<sup>53</sup> such as the mechanical properties of

the substrate, the milling intensity is expected to be proportional to the kinetic energy of the ball ( $KE_{ball}$ ) and collision frequency ( $f_{coll}$ ) (**Equation 6**). In a system with a single milling ball, the velocity component of the kinetic energy and the collision frequency can be expected to be linearly proportional to the milling frequency ( $f_{mill}$ ). From these assumptions, an expression for the conversion with respect to time ( $X(t)$ ) can be derived (**Equation 7**) based on the BPR and milling frequency of the specific reaction and an apparent rate constant ( $k'$ ).

$$\frac{dX}{dt} = k \cdot I_m \quad (5)$$

$$I_m \propto \frac{KE_{ball} \cdot f_{coll}}{m_{substrate}} \propto \frac{m_{ball}}{m_{substrate}} f_{mill}^3 \quad (6)$$

$$X(t) = k' \cdot BPR \cdot f_{mill}^3 \cdot t \quad (7)$$

Furthermore, plotting the depolymerization curves for the different ball densities against time multiplied by the BPR shows that the linear relationship between conversion and BPR holds true during the initial portion of the reaction for the stainless steel and aluminum oxide balls (**Figure 6a**). The depolymerization rate using a tungsten carbide ball, however, does deviate from this trend. Similar to the very low BPR, a non-linear response in the material properties of the substrate may also exist at significantly higher BPRs that could explain this discrepancy. When the depolymerization curves between the 30 Hz, 27.5 Hz, and 25 Hz are plotted as a function time multiplied by the frequency cubed, the initial conversions nearly perfectly overlap (**Figure 6b**). This confirms the cubed relationship between milling frequency and conversion.

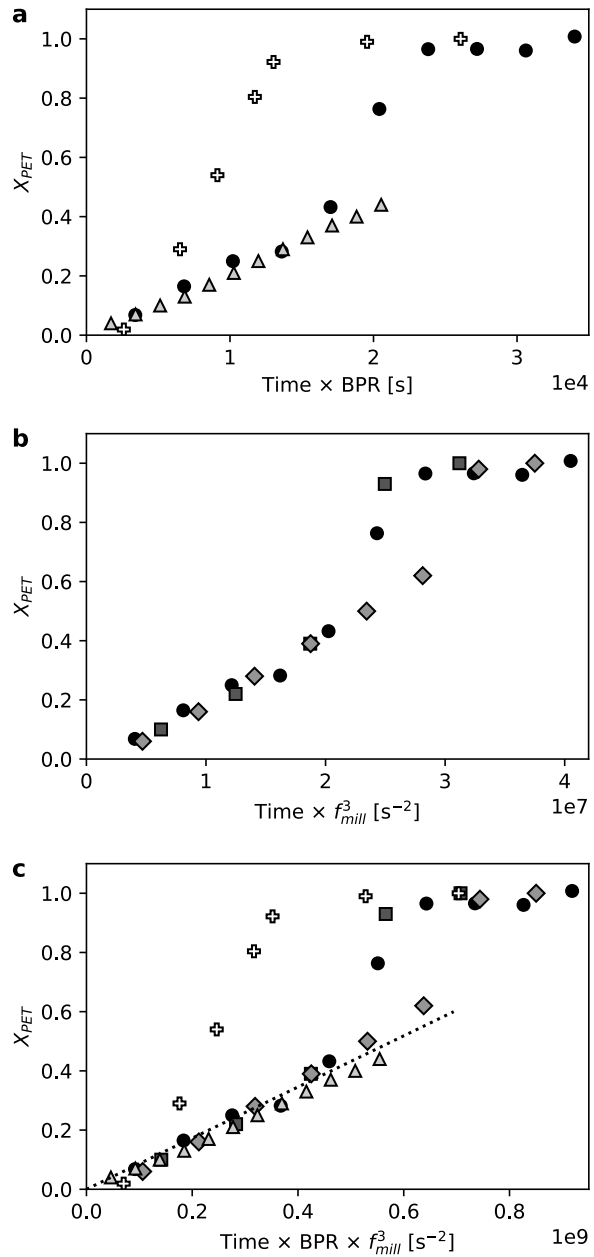


**Figure 6.** (a) Conversion of PET milled with a 20 mm stainless-steel (S.S.) (●), tungsten carbide (✚), and aluminum oxide (▲) ball at 30 Hz. (b) Conversion of PET milled with a 20 mm S.S. ball at 30 Hz (●), 27.5 Hz (■), and 25 Hz (◆). (c) Conversion of PET under all five conditions. Dashed line is modeled conversion based on the fit  $k'$ .

Finally, plotting all five datasets on a similarly scaled time axis shows the invariance of conversion when accounting for the BPR and milling frequency (**Figure 6c**), validating **Equation 7** within the explored parameter space. The apparent rate constant ( $k'$ ) was determined to be  $8.6 \pm 0.5 \times 10^{-10} \text{ s}^2$  by averaging the slope of the best-fit line for the datasets, excluding the tungsten carbide. The capability of the energetics of the system to describe the reaction progression further supports the energy-driven shrinking core model described above. Future work will be necessary to further deconvolute the system variables that comprise  $k'$  to develop a more generalized model, as well as further exploring the relationship between BPR and conversion to account for more extreme cases. Finally, additional terms to describe the occurrence of the inflection point are needed to fully describe the reaction. However, this confirmation that the milling energy is the dominant descriptor of the system will be an important jumping-off point when trying to model and describe this reaction in more complex systems that more closely resemble industrial conditions, such as in a planetary ball mill.

## CONCLUSIONS

Balling milling PET with NaOH can achieve complete depolymerization to sodium terephthalate and ethylene glycol within 20 minutes. The process occurs in two distinct stages. In the first stage, the conversion increases linearly with milling time. For a single-ball system, the initial rate of depolymerization scales with the number and kinetic energy of the collision. Thus, it is proportional to the mass of the ball and the third power of the milling frequency. There is also correlation between conversion and ball-to-reactant mass ratio for single-ball experiments suggesting that the extent of reaction scales with energy dose.

Once the conversion reaches approximately 40%, the feedstock mixture transforms from a fine powder to a dense wax, and the rate of conversion increases significantly until complete conversion

is achieved. This is attributed to a more effective energy transfer to the reactants during collisions. The molecular weight distribution (MWD) curve becomes slightly narrower as the reaction progresses while representing a decreasing amount of residual PET. This implies that specific polymers chains are depolymerized completely once they are affected by a collision. The reaction kinetics can be explained by a modified shrinking core model in which the energy transfer or interfacial contacting induced by collisions rather than diffusion of a reactant is the limiting factor.

The temperature influences the PET depolymerization reaction in a complex way, which may be related to contributions of thermal energy, changes in mechanical properties of the polymer and transport of reactants to the interface.

## ASSOCIATED CONTENT

### **Supporting Information.**

The Supporting Information is available free of charge on the ACS Publications website at DOI:  
10.xxxx

The Supporting Information includes the NMR results and discussion, results from elemental analysis, and additional GPC results.

## AUTHOR INFORMATION

### **Corresponding Author**

\* Tel: +1 (404) 385-7685. Email: carsten.sievers@chbe.gatech.edu

### **Author Contributions**

The manuscript was written through contributions of all authors. All authors have given approval to the final version of the manuscript.

## ACKNOWLEDGMENT

The work was financially supported by Kolon Industries, Inc. through the Kolon Center for Lifestyle Innovation at Georgia Tech and the U.S. National Science Foundation - Emerging Frontiers in Research and Innovation program under grant 2028998.

## ABBREVIATIONS

PET, poly(ethylene terephthalate); Na<sub>2</sub>TPA, disodium terephthalate; EG, ethylene glycol; M<sub>N</sub>, number average molecular weight; M<sub>w</sub>, weight average molecular weight, MWD, molecular weight distribution; S.S., stainless-steel; BPR, ball-to-powder ratio

## REFERENCES

1. Barnard, E.; Arias, J. J. R.; Thielemans, W., Chemolytic depolymerisation of PET: a review. *Green Chem.* **2021**, *23*, 3765-3789; 10.1039/d1gc00887k
2. Smith, O.; Brisman, A., Plastic Waste and the Environmental Crisis Industry. *Crit. Criminol.* **2021**, *29*, 289-309; 10.1007/s10612-021-09562-4
3. Tiso, T.; Narancic, T.; Wei, R.; Pollet, E.; Beagan, N.; Schroder, K.; Honak, A.; Jiang, M.; Kenny, S. T.; Wierckx, N.; Perrin, R.; Averous, L.; Zimmermann, W.; O'Connor, K.; Blank, L. M., Towards bio-upcycling of polyethylene terephthalate. *Metab. Eng.* **2021**, *66*, 167-178; 10.1016/j.ymben.2021.03.011
4. Geyer, R.; Jambeck, J. R.; Law, K. L., Production, use, and fate of all plastics ever made. *Sci. Adv.* **2017**, *3*, e1700782; 10.1126/sciadv.1700782
5. Stahel, W. R., The circular economy. *Nature* **2016**, *531*, 435-8; 10.1038/531435a
6. Nikles, D. E.; Farahat, M. S., New motivation for the depolymerization products derived from poly(ethylene terephthalate) (PET) waste: A review. *Macromol. Mater. Eng.* **2005**, *290*, 13-30; 10.1002/mame.200400186

7. Sinha, V.; Patel, M. R.; Patel, J. V., Pet Waste Management by Chemical Recycling: A Review. *J. Polym. Environ.* **2010**, *18*, 8-25; 10.1007/s10924-008-0106-7

8. Ryberg, M. W.; Hauschild, M. Z.; Wang, F.; Averous-Monnery, S.; Laurent, A., Global environmental losses of plastics across their value chains. *Resour. Conserv. Recycl.* **2019**, *151*, 104459; 10.1016/j.resconrec.2019.104459

9. Lundell, C.; Thomas, J. In *PET: Polyethylene Terephthalate – The Ubiquitous 500 ml Water Bottle*, International Conference on Applied Human Factors and Ergonomics, Cham, Springer International Publishing: Cham, 2020; pp 248-254.

10. Khoonkari, M.; Haghghi, A. H.; Sefidbakht, Y.; Shekoohi, K.; Ghaderian, A., Chemical Recycling of PET Wastes with Different Catalysts. *Int. J. Polym. Sci.* **2015**, *2015*, 124524; 10.1155/2015/124524

11. Karayannidis, G. P.; Chatziavgoustis, A. P.; Achilias, D. S., Poly(ethylene terephthalate) recycling and recovery of pure terephthalic acid by alkaline hydrolysis. *Adv. Polym. Technol.* **2002**, *21*, 250-259; 10.1002/adv.10029

12. La Mantia, F. P.; Vinci, M., Recycling poly(ethyleneterephthalate). *Polym. Degrad. Stab.* **1994**, *45*, 121-125; 10.1016/0141-3910(94)90187-2

13. Eriksen, M. K.; Christiansen, J. D.; Daugaard, A. E.; Astrup, T. F., Closing the loop for PET, PE and PP waste from households: Influence of material properties and product design for plastic recycling. *Waste Manag.* **2019**, *96*, 75-85; 10.1016/j.wasman.2019.07.005

14. Guclu, G.; Kasgoz, A.; Ozbudak, S.; Ozgumus, S.; Orbay, M., Glycolysis of poly(ethylene terephthalate) wastes in xylene. *J. Appl. Polym. Sci.* **1998**, *69*, 2311-2319; 10.1002/(SICI)1097-4628(19980919)69:12<2311::AID-APP2>3.0.CO;2-B

15. Campanelli, J. R.; Kamal, M. R.; Cooper, D. G., Kinetics of Glycolysis of Poly(Ethylene-Terephthalate) Melts. *J. Appl. Polym. Sci.* **1994**, *54*, 1731-1740; 10.1002/app.1994.070541115

16. Yoshioka, T.; Motoki, T.; Okuwaki, A., Kinetics of hydrolysis of poly(ethylene terephthalate) powder in sulfuric acid by a modified shrinking-core model. *Ind. Eng. Chem. Res.* **2001**, *40*, 75-79; DOI 10.1021/ie000592u

17. Campanelli, J. R.; Cooper, G.; Kamal, M. R., Catalyzed-Hydrolysis of Polyethylene Terephthalate Melts. *J. Appl. Polym. Sci.* **1994**, *53*, 985-991; 10.1002/app.1994.070530801

18. Vaidya, U. R.; Nadkarni, V. M., Unsaturated Polyesters from Pet Waste - Kinetics of Polycondensation. *J. Appl. Polym. Sci.* **1987**, *34*, 235-245; 10.1002/app.1987.070340120

19. Güçlü, G.; Yalçınova, T.; Özgümüş, S.; Orbay, M., Hydrolysis of waste polyethylene terephthalate and characterization of products by differential scanning calorimetry. *Thermochim. Acta* **2003**, *404*, 193-205; 10.1016/s0040-6031(03)00160-6

20. Campanelli, J. R.; Kamal, M. R.; Cooper, D. G., A Kinetic-Study of the Hydrolytic Degradation of Polyethylene Terephthalate at High-Temperatures. *J. Appl. Polym. Sci.* **1993**, *48*, 443-451; 10.1002/app.1993.070480309

21. Pitat, J.; Holcik, V.; Bacak, M. A method of processing waste of polyethylene terephthalate by hydrolysis. 1959.

22. Kao, C. Y.; Cheng, W. H.; Wan, B. Z., Investigation of alkaline hydrolysis of polyethylene terephthalate by differential scanning calorimetry and thermogravimetric analysis. *J. Appl. Polym. Sci.* **1998**, *70*, 1939-1945; Doi 10.1002/(Sici)1097-4628(19981205)70:10<1939::Aid-App8>3.0.Co;2-G

23. Anwar, J.; Munawar, M. A.; Abbas, Z.; Anzano, J. M., Production of Terephthalic Acid from Waste Polyethylene Terephthalate) Materials. *J. Polym. Eng.* **2008**, *28*, 129-140; <https://doi.org/10.1515/POLYENG.2008.28.3.129>

24. Wu, H.-S., Strategic possibility routes of recycled PET. *Polymers* **2021**, *13*, 1475; 10.3390/polym13091475

25. Crippa, M.; Morico, B., PET depolymerization: a novel process for plastic waste chemical recycling. In *Catalysis, Green Chemistry and Sustainable Energy*, Basile, A.; Centi, G.; Falco, M. D.; Iaquaniello, G., Eds. Elsevier: 2020; Vol. 179, pp 215-229.

26. Calvaruso, G.; Clough, M. T.; Rechulski, M. D. K.; Rinaldi, R., On the meaning and origins of lignin recalcitrance: A critical analysis of the catalytic upgrading of lignins obtained from mechanocatalytic biorefining and organosolv pulping. *ChemCatChem* **2017**, *9*, 2691-2700; <https://doi.org/10.1002/cctc.201700473>

27. Schüth, F.; Rinaldi, R.; Meine, N.; Käldström, M.; Hilgert, J.; Rechulski, M. D. K., Mechanocatalytic depolymerization of cellulose and raw biomass and downstream processing of the products. *Catal. Today* **2014**, *234*, 24-30; 10.1016/j.cattod.2014.02.019

28. Zhang, Q.; Jerome, F., Mechanocatalytic Deconstruction of Cellulose: An Emerging Entry into Biorefinery. *ChemSusChem* **2013**, *6*, 2042-2044; <https://doi.org/10.1002/cssc.201300765>

29. Kessler, M.; Woodward, R. T.; Wong, N.; Rinaldi, R., Kinematic Modeling of Mechanocatalytic Depolymerization of alpha-Cellulose and Beechwood. *ChemSusChem* **2018**, *11*, 552-561; 10.1002/cssc.201702060

30. Hick, S. M.; Griebel, C.; Restrepo, D. T.; Truitt, J. H.; Buker, E. J.; Bylda, C.; Blair, R. G., Mechanocatalysis for biomass-derived chemicals and fuels. *Green Chem.* **2010**, *12*, 468-474; 10.1039/b923079c

31. Calvaruso, G.; Clough, M. T.; Rinaldi, R., Biphasic extraction of mechanocatalytically-depolymerized lignin from water-soluble wood and its catalytic downstream processing. *Green Chem.* **2017**, *19*, 2803-2811; 10.1039/c6gc03191a

32. Kleine, T.; Buendia, J.; Bolm, C., Mechanochemical degradation of lignin and wood by solvent-free grinding in a reactive medium. *Green Chem.* **2013**, *15*, 160-166; 10.1039/c2gc36456e

33. Brittain, A. D.; Chrisandina, N. J.; Cooper, R. E.; Buchanan, M.; Cort, J. R.; Olarte, M. V.; Sievers, C., Quenching of Reactive Intermediates during Mechanochemical

Depolymerization of Lignin. *Catal. Today* **2018**, *302*, 180-189;  
<https://www.sciencedirect.com/science/article/pii/S0920586117302997>

34. Yabushita, M.; Kobayashi, H.; Kuroki, K.; Ito, S.; Fukuoka, A., Catalytic Depolymerization of Chitin with Retention of N-Acetyl Group. *ChemSusChem* **2015**, *8*, 3760-3; 10.1002/cssc.201501224

35. Hewlett, P.; Liska, M., Clinker Grinding. In *Lea's Chemistry of Cement and Concrete*, 5th edition ed.; Elsevier: 2019; pp 52 - 56.

36. Drahla, C. Plastics Recycling with Microbes and Worms is Further Away than People Think. <https://cen.acs.org/environment/sustainability/Plastics-recycling-microbes-worms-further/96/i25> (accessed April 18, 2021).

37. Wei, R.; Zimmermann, W., Microbial enzymes for the recycling of recalcitrant petroleum-based plastics: how far are we? *Microb. Biotechnol.* **2017**, *10*, 1308-1322; 10.1111/1751-7915.12710

38. Li, Y.; Yi, H.; Ge, M.; Yao, D., Scale-Up Synthesis of High Purity Calcium Terephthalate from Polyethylene Terephthalate Waste: Purification, Characterization, and Quantification. *Macromol. Mater. Eng.* **2021**, *306*, 2100591; 10.1002/mame.202100591

39. Li, Y. Y.; Yao, D. G.; Ge, M. Q., Reactive melt processing of poly(ethylene terephthalate) waste into calcium terephthalate. *Express Polym. Lett.* **2021**, *15*, 153-165; 10.3144/expresspolymlett.2021.14

40. Štrukil, V., Highly efficient solid-state hydrolysis of waste polyethylene terephthalate by mechanochemical milling and vapour-assisted aging. *ChemSusChem* **2021**, *14*, 330-338; 10.1002/cssc.202002124

41. Giraud, M.; Gatamel, C.; Vaudez, S.; Nos, J.; Gervais, T.; Bernard-Granger, G.; Berthiaux, H., Investigating grinding mechanisms and scaling criteria in a ball mill by dimensional analysis. *Adv. Powder Technol.* **2021**, *32*, 2988-3001; 10.1016/j.apt.2021.06.016

42. Burgio, N.; Iasonna, A.; Magini, M.; Martelli, S.; Padella, F., Mechanical alloying of the Fe–Zr system. Correlation between input energy and end products. *Il Nuovo Cimento D* **1991**, *13*, 459-476; 10.1007/bf02452130

43. Suryanarayana, C., Mechanical alloying and milling. *Prog. Mater. Sci.* **2001**, *46*, 1-184; 10.1016/S0079-6425(99)00010-9

44. Odain, G., Step Polymerization. In *Principles of Polymerization*, Odain, G., Ed. 2004; pp 39-197.

45. Kumar, S.; Guria, C., Alkaline hydrolysis of waste poly(ethylene terephthalate): A modified shrinking core model. *J. Macromol. Sci. A* **2005**, *A42*, 237-251; 10.1081/Ma-200050346

46. López-Fonseca, R.; González-Velasco, J.; Gutiérrez-Ortiz, J., A shrinking core model for the alkaline hydrolysis of PET assisted by tributylhexadecylphosphonium bromide. *Chem. Eng. J.* **2009**, *146*, 287-294; 10.1016/j.cej.2008.09.039

47. Fogler, H. S., The Shrinking Core Model. In *Elements of Chemical Reaction Engineering*, 3rd Ed., 3 ed.; Fogler, H. S., Ed. 1999; pp 719-727.

48. Hutchings, B. P.; Crawford, D. E.; Gao, L.; Hu, P.; James, S. L., Feedback Kinetics in Mechanochemistry: The Importance of Cohesive States. *Angew. Chem. Int. Edit.* **2017**, *56*, 15252-15256; 10.1002/anie.201706723

49. Bai, C.; Spontak, R. J.; Koch, C. C.; Saw, C. K.; Balik, C. M., Structural changes in poly(ethylene terephthalate) induced by mechanical milling. *Polymer* **2000**, *41*, 7147-7157; 10.1016/S0032-3861(00)00048-3

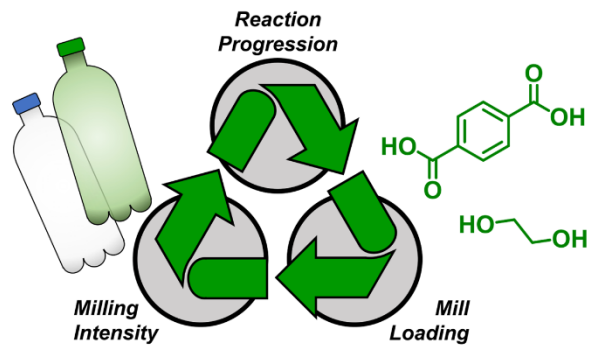
50. Allen, N. S.; Edge, M.; Mohammadian, M.; Jones, K., Hydrolytic Degradation of Poly(Ethylene-Terephthalate) - Importance of Chain Scission Versus Crystallinity. *Eur. Polym. J.* **1991**, *27*, 1373-1378; 10.1016/0014-3057(91)90237-I

51. Stearne, J. M.; Ward, I. M., The tensile behaviour of polyethylene terephthalate. *J. Mater. Sci.* **1969**, *4*, 1088-1096; 10.1007/bf00549849

52. Delogu, F.; Mulas, G.; Schiffini, L.; Cocco, G., Mechanical work and conversion degree in mechanically induced processes. *Mater. Sci. Eng. A* **2004**, 382, 280-287; 10.1016/j.msea.2004.05.047

53. Tricker, A. W.; Samaras, G.; Hebisch, K. L.; Realff, M. J.; Sievers, C., Hot spot generation, reactivity, and decay in mechanochemical reactors. *Chem. Eng. J.* **2020**, 382, 122954; 10.1016/j.cej.2019.122954

For Table of Contents Use Only.



The reaction stages during the rapid mechanochemical depolymerization of poly(ethylene terephthalate) are described and the influence of milling parameters on the kinetics are explored.